Toward Molecular Textiles: Synthesis and Characterization of Molecular Patches

Camiel C. E. Kroonen,[a] Antoine Hinaut,[b] Adriano D'Addio,[a] Alessandro Prescimone,[a] Daniel Häussinger,[a] Gema Navarro-Marín,[b] Olaf Fuhr,[c] Dieter Fenske,[c] Ernst Meyer,[b] and Marcel Mayor*[a, c, d]

In memory of the pioneer of covalent templating Prof. Dr. Gottfried Schill

This works describes a new step into the assembly of molecular textiles by the use of covalent templating. To establish a well-founded base and to tackle pre-mature obstacles, expected during the fabrication of the desired 2D-material, we opted to investigate the in-solution synthesis of molecular patches e.g. cut-outs of a textile. A bi-functional cross-shaped monomer was designed, synthesized and was in-detail characterized by means of ^{1}H-NMR and chiro-optical spectroscopy. In addition, x-ray structure crystallography was used to assess the absolute configuration. The monomer was used in an in-solution oligomerization to assemble the molecular patches via imine condensation, which revealed the formation of predominately dimeric patches. The imine-oligomer mixtures were further analyzed by reduction and cleaved to investigate the conditions required post mono-layer assembly. All reaction stages were followed by FT-IR and ^{1}H-NMR analysis. Finally, we address the adsorption of the cross-shaped monomer onto a Au(111) surface, via high vacuum electrospray deposition. The subsequent annealing of the interface induced the on-surface imine condensation reaction, leading to unidimensional oligomers co-adsorbed with clusters of cyclic-dimers. Nc-AFM analysis revealed the tridimensional molecular structures, and together with electrospray deposition technique showed to be a promising pathway to investigate potential monomer candidates.

Introduction

Interweaving structures is a craft humankind has mastered long ago, with as prime example the invention of textiles and fabrics.[1] These type of materials are indispensable in nowadays society due to the features they combine: flexibility and comfort with strength and endurability.[2] Mimicking interwoven materials on the molecular scale is a scientific challenge addressing intriguing questions like: "how do the advantageous macro-scopic features translate to the nano-scale level?" and even before that, "how can we interweave molecular architectures in a controlled manner?".[3]

Catenanes and rotaxanes were the first reported mechanically interlocked structures, resulting in the rapid exploration of a multitude of sophisticated frameworks.[4–8] The challenge in many of these thermodynamically controlled assemblies is to have access to suitable building blocks that combine dynamic features, pre-organization as well as synthetic availability. It was found that many of the chemical designs use either supramolecular interactions or metal coordinated templates. Nevertheless, the first ever templated assembly of a catenane, reported by Schill and Lütringhaus, was done via a covalent templating strategy.[9] Even though metal coordinated building blocks have in many cases out-performed covalent template strategies, there are a few examples of high-yielding covalent template based approaches.[10,11]

A special class of molecular interwoven materials, as mentioned before, are molecular- textiles and fabrics. The simplest molecular textiles, consisting of two-dimensional braided linear polymer chains, are a new class of 2D materials that have gotten some attention in the last years.[2,3,12] In this area of expertise there are some examples based on metal-coordinated or supramolecular assembled structures.[13–15] However, there is no proven example of a fully organic covalent templating approach yet. In our recent work, we shared our new strategy for fabricating molecular textiles based on a cross-shaped monomer that retains its conformation via a covalent

[a] C. C. E. Kroonen, A. D'Addio, A. Prescimone, D. Häussinger, M. Mayor
Department of Chemistry, University of Basel, St. Johanns-Ring 19, 4056 Basel, (Switzerland)
E-mail: marcel.mayor@unibas.ch

[b] A. Hinaut, G. Navarro-Marín, E. Meyer
Department of Physics, University of Basel, Klingelbergstrasse 82, 4056 Basel, (Switzerland)

[c] O. Fuhr, D. Fenske, M. Mayor
Institute for Nanotechnology (INT) and Karlsruhe Nano Micro Facility (KNMFi), Karlsruhe Institute of Technology (KIT), P. O. Box 3640, 76021 Karlsruhe Eggenstein-Leopoldshafen, (Germany)

[d] M. Mayor
Lehn Institute of Functional Materials(LIFM), School of Chemistry, Sun Yat-Sen University (SYSU), Guangzhou 510275, (P.R. of China)

Chem. Eur. J. 2024, 30, e202402866 (1 of 12)

© 2024 The Author(s). Chemistry - A European Journal published by Wiley-VCH GmbH

Chemistry–A European Journal

Research Article
doi.org/10.1002/chem.202402866

Chemistry Europe
European Chemical
Societies Publishing

template.[16] Assembly of this monomer on the air-water interface, should yield a 2D cross-linked network that is the precursor towards a molecular textile. Initial results have shown promising trends, but also classified characterization of this mono-layer thick material, as extremely challenging. In order to build a well-founded base for understanding the molecular structure and to fully comprehend the chemistry applied, we hypothesized about an in-solution strategy towards molecular patches. In-solution assembly of a textile cut-out would allow to mimic the fabrication procedure of our target textile and in addition provide us with a small structural analogue. Thereby, the outcome of this investigation will provide us with essential information with regard to reactivity, synthetic strategy and helps us to pin-point analysis.

In this work, we describe the synthesis of a fully-organic cross-shaped bi-functional monomer that can be used to assemble molecular patches. This monomer, functionalized with a benzylic amine and aldehyde, can be used in wet-chemistry set-ups and can be analyzed with conventional organic synthesis analysis techniques. Furthermore, we report the in-solution oligomerization via imine condensation as well as the on-surface synthesis and characterization of linear and cyclic oligomers.

Results and Discussion

Design & Retrosynthesis

Our previous reported approach in the exploration of a new route towards molecular textiles is shown in the left side of Figure 1. Here, the monomers are cross-shaped, consisting of a pair of rigid-rod type structures as bars which are geometrically arranged b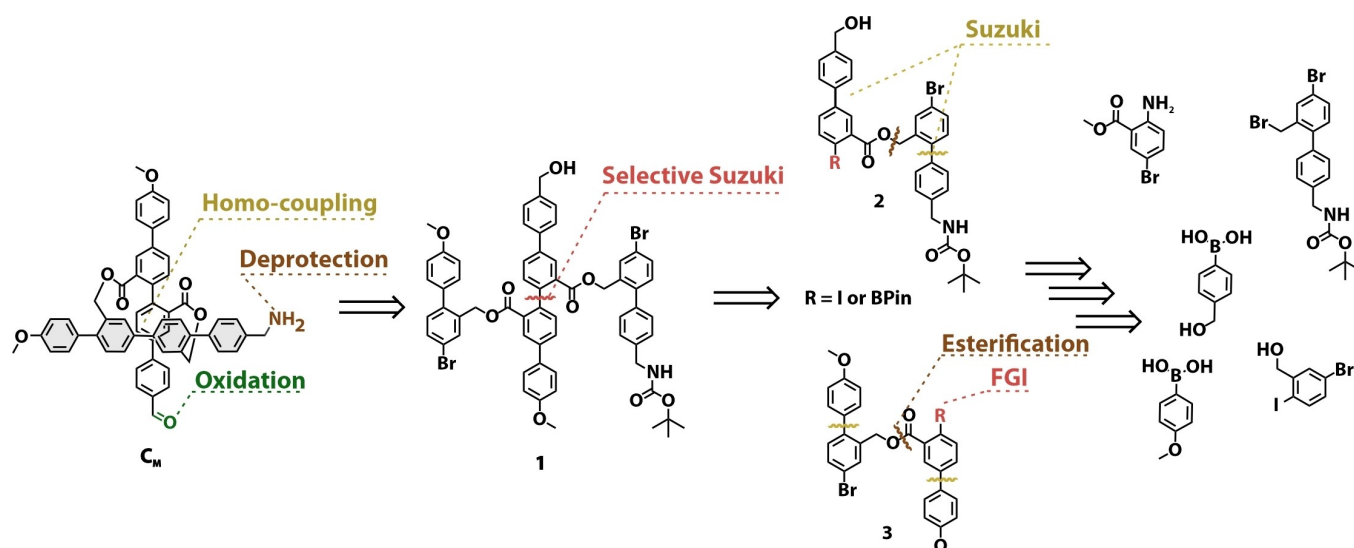y a covalent template. The control over both, the orientation of the cross-shaped monomer at the air/water interface and the functional groups exposed at the ends of the bars should enable the formation of the molecular textile. Thereby, the monomers represent the cross-over points of the textile and are assembled in a monolayer structure at the air/water interface. After template cleavage, the monolayer should yield in two perpendicular sets of parallel and periodically interwoven linear polymer strands: the molecular textile.

To make the system more processible we focus on a structural analogue, namely the investigation of a cut-out of the textile, e.g. 2×2 grid (depicted in purple). This pathway would allow to investigate the polymerization in wet chemistry, while characterizable by conventional analysis techniques like ^{1}H-NMR and IR. Additionally, it would allow to tackle pre-mature processing challenges that we envision to do post mono-layer assembly e.g. imine reduction or template cleavage. In addition, the molecular patch would be a semi-interwoven resemblance of a textile, that could be investigated on mono-layer scale to pin-point structural and chemical characterization by e.g. atomic force microscopy (AFM). Figure 1, on the right section depicts the molecular design of an asymmetric analogue C_M, of our early reported envisioned cross-shaped monomers. Here, a terminus of each para-quarterphenyl rod forming the cross-shaped monomer is 'blocked' as an unreactive methoxy group, while the other end resembles the benzylic amine and aldehyde functionality intended for use in the imine condensation.

In Scheme 1, the retro-synthetic analysis of bi-functional asymmetric monomer C_M is depicted. The target structure was envisioned to be obtained, similar to our reported strategy, in a late stage from 1 via an oxidative homo-coupling macro-cyclization followed by oxidation to the aldehyde and deprotection of the Boc-group. Key intermediate 1, should be accessible via a selective Suzuki-cross coupling reaction of precursor 2 and 3, profiting from the reactivity difference
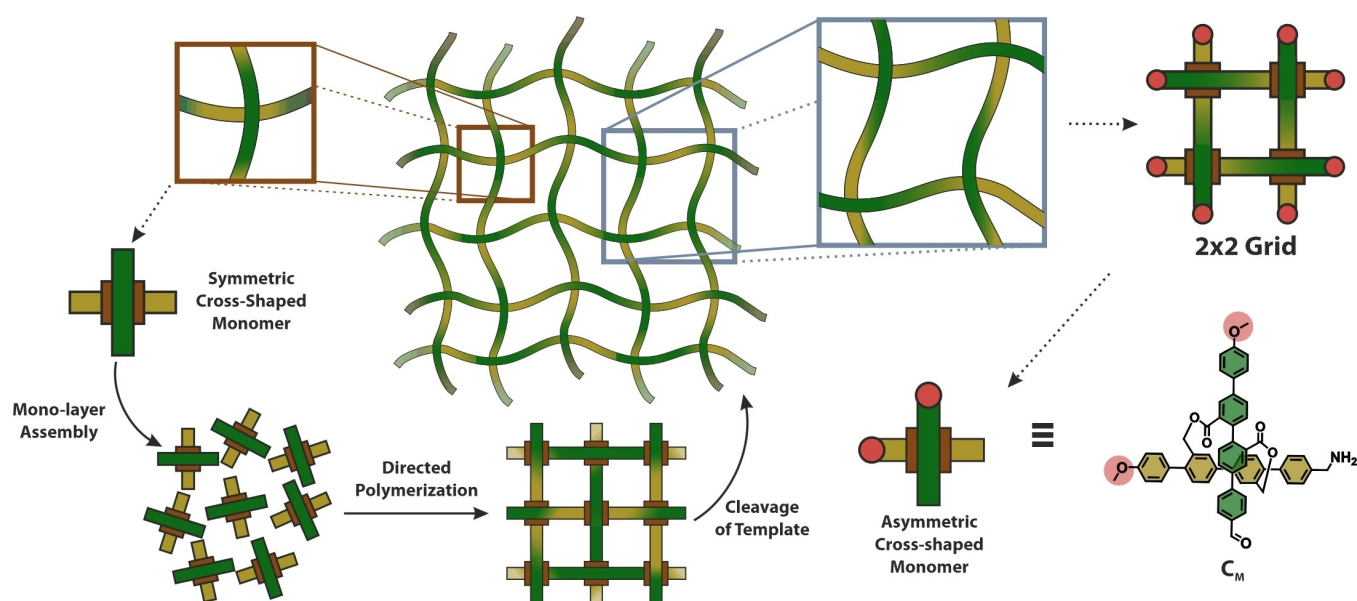
Figure 1. left) Schematic illustration of bottom-up approach of synthesizing a molecular textile utilizing the preorganization of a symmetric cross-shaped monomer at the air-water interface right) Schematic visualization of a cut-out of the molecular textile (2×2 grid) and the molecular design of a bi-functional asymmetric monomer C_M that via imine condensation could assemble into cyclic oligomers.

Chemistry–A European Journal

Research Article
doi.org/10.1002/chem.202402866

Chemistry Europe
European Chemical
Societies Publishing

Scheme 1. Retrosynthetic analysis: Assembly of asymmetric cross-shaped monomer **C$_M$**.

between an aryl-iodine and an aryl-bromine with regard to palladium catalyzed cross-coupling chemistry.[17] Here, it was envisioned that either **2** or **3** could be selectively converted from an aryl-iodide to a bis-pinacolato borane via a *Miyaura* borylation. The building block **2**, with the benzylic alcohol and masked amine functionality as well as **3** containing the methoxy groups could be assembled from similar precursors via series of well-established reactions like *Sandmeyer* functional group conversion, *Suzuki* cross-coupling reaction and esterification.
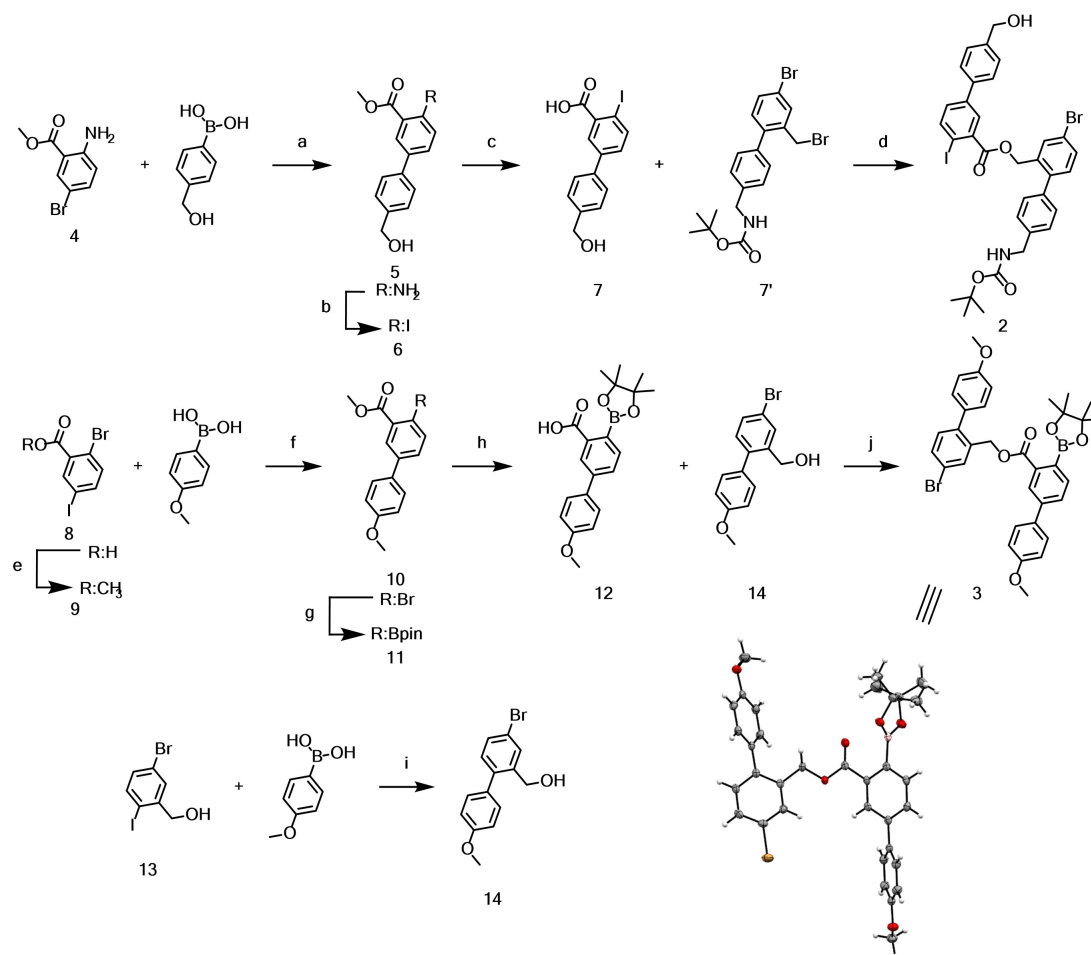
Synthesis

The synthesis of **C$_M$** started with the assembly of intermediates **2** and **3**, shown in Scheme 2. Building block **2** was obtained in 4 steps from 2-amino 5-bromo benzoate **4**. First, **4** was reacted with [4-(hydroxymethyl)phenyl]boronic acid in a *Suzuki* cross-coupling reaction to obtain **5** in moderate yield. The amine was converted to iodide **6** in excellent yields (90%), utilizing a *Sandmeyer*-iodination with para-toluene sulfonic acid (p-TsOH), sodium nitrite (NaNO$_2$) and potassium iodide (KI) in a mixture of acetonitrile (ACN) and water. Saponification of the ester yielded **7**, which was reacted with previously reported **7'** in a cesium fluoride mediated substitution reaction to yield ester **2** in almost quantitative yield over two steps.[16] With **2** in hand the selective borylation of the aryl-iodide was attempted, however this turned out to be unexpectedly challenging. Under a range of attempted *Miyaura* conditions, ranging from mild to harsher, there was almost no conversion or resulted in predominately dehalogenated products. Therefore, the strategy to assemble key intermediate **3** was slightly adapted by introducing the boronic ester in an earlier stage. Acid **8** was methyl-protected via *Fischer* esterification, followed by a selective *Suzuki*-cross coupling of **9** with [4-(methoxy)phenyl]boronic acid to yield **10** in moderate yield. The aryl-bromide was converted to boronic ester **11**, via *Miyaura*-borylation conditions with PdCl$_2$(dppf),

bis-(pinacolato borane) (B$_2$Pin$_2$) and potassium acetate (KOAc) in dioxane at elevated temperature. Acid **12** was obtained quantitatively from **11** upon saponification with lithium hydroxide in a tetrahydrofuran water mixture. Benzylic alcohol **14** was obtained via a selective *Suzuki* cross-coupling from (5-bromo-2-iodophenyl)methanol **13** and successfully coupled to **12** via *Steglich* esterification utilizing dicyclohexyl carbodiimide (DCC) and 4-dimethylaminopyridine (DMAP) yielding **3**. The identity of **3** was corroborated by its solid-state structure. Single crystals suitable for X-ray analysis were obtained by slow evaporation of the solvent from a solution of **3** in CD$_2$Cl$_2$.

Scheme 3 shows how the previously prepared building blocks **2** and **3** were coupled via a selective *Suzuki* cross-coupling at moderate temperature to yield key intermediate di-bromide **1** in good yield. In a next step the bromines were converted to boronic esters via *Miyaura* borylation and the obtained crude was directly exposed to palladium mediated oxidative homo-coupling conditions. This key macro-cyclization step provided **C$_1$** in excellent yields (64%) over both steps. By late stage modifications, **C$_2$** was obtained upon oxidation of the alcohol to the aldehyde by *Dess-Martin* periodane (DMP), which was quantitatively converted to **C$_M$** by exposure to trifluoro-acetic acid (TFA) in dichloromethane. The target monomer **C$_M$** was obtained as it's TFA-salt after co-evaporation of residual TFA with toluene. All compounds were accessible in good quality without excessive purification protocols and where characterized by ^{1}H-NMR, ^{13}C-NMR and HR-ESI-MS.
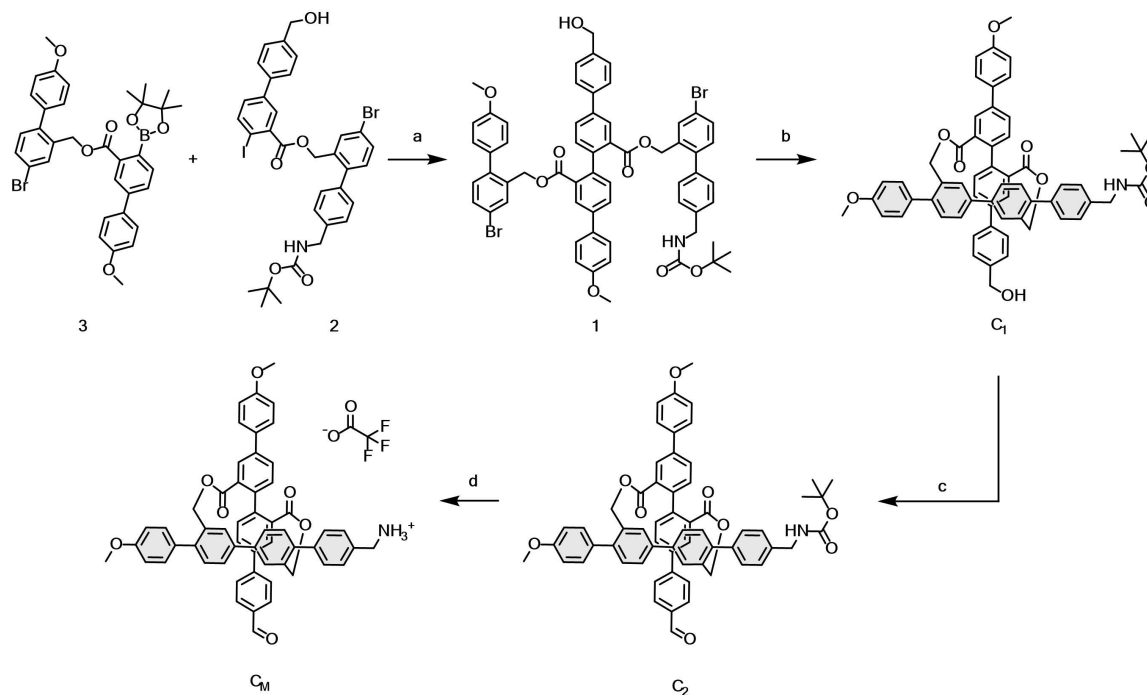
Physicochemical Analysis

The ^{1}H-NMR analysis of final cross **C$_2$** displayed interesting features. First of all, it showed the formation of the rigid cross-shape structure due to the presence of the diastereotopic protons observed before (Figure 2), which correspond to the benzylic ester protons.[16] Due to the lack of symmetry in **C$_2$**

Chemistry–A European Journal

Research Article
doi.org/10.1002/chem.202402866

Chemistry
Europe
European Chemical
Societies Publishing

Scheme 2. Synthesis of precursors **2** and **3**. Conditions: a) Pd(PPh$_3$)$_4$; Na$_2$CO$_3$; Tol/MeOH/H$_2$O (4:1:1.5); 80 °C; 5 h; 65 %. b) p-TsOH; NaNO$_2$; KI; ACN/H$_2$O (3:1); 0 °C-r.t.; 16 h; 90 %. c) NaOH; MeOH/H$_2$O; reflux; 3 h; 98 %. d) **7′**; CsF; DMF; r.t.; 16 h; 99 % e) H$_2$SO$_4$; MeOH; reflux; 4 h; 85 % f) PdCl$_2$(dppf); K$_2$CO$_3$; DME/MeOH/H$_2$O (4:1:1); 65 °C; 16 h; 71 %. g) PdCl$_2$(dppf); B$_2$Pin$_2$; KOAc; dioxane; 90 °C; 6 h; 85 %. h) LiOH; THF/H$_2$O; r.t.; 1 h; quant. i) PdCl$_2$(dppf); K$_2$CO$_3$; DME/H$_2$O (4:1); 60 °C; 3 h; 87 %. j) **14**; DCC; DMAP; CH$_2$Cl$_2$/DMF; r.t.; 1.5 h; 44 %. Bottom-right) Solid-state structure of **3** plotted as ORTEP plots with 50 % probability.
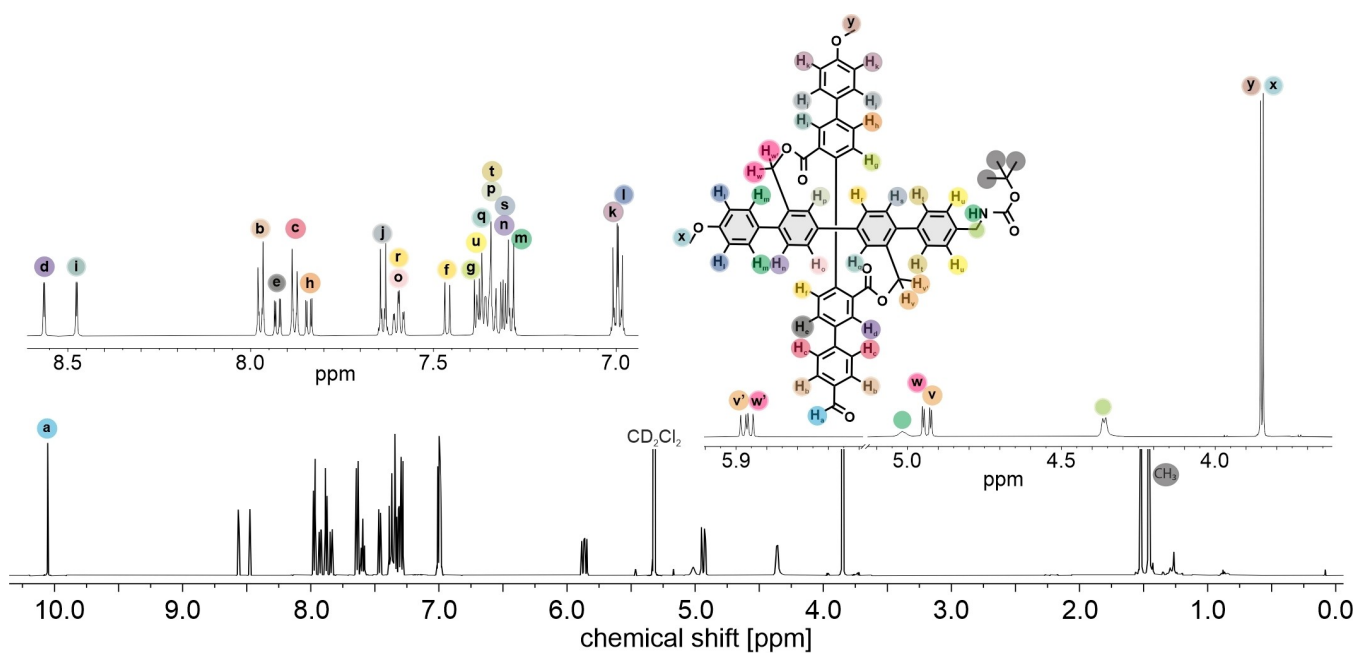
**Figure 2.** ^{1}H-NMR spectra of **C$_2$** in CD$_2$Cl$_2$ with assignment of the corresponding signals (600 mHz, 25 °C).

Chemistry–A European Journal

Research Article
doi.org/10.1002/chem.202402866

Chemistry
Europe
European Chemical
Societies Publishing

Scheme 3. Synthesis of **C$_M$**. Conditions: a) PdCl$_2$(dppf); K$_2$CO$_3$; THF/H$_2$O (4:1); 60°C; 5 h; 82%. b) i] PdCl$_2$(dppf); B$_2$Pin$_2$; KOAc; dioxane; 90°C; 4 h; ii] PdCl$_2$(PPh$_3$)$_2$; THF/H$_2$O (9:1); r.t.; 16 h; 64% two steps. c) DMP; CH$_2$Cl$_2$; 0°C-r.t.; 2 h; 86%; d) TFA; CH$_2$Cl$_2$; r.t.; 1 h; quant.

there are two sets of doublets for these protons (H$_v$ and H$_w$). The dissymmetry is further displayed in the separation of almost equivalent protons, *e.g.* the two methoxy CH$_3$ singlets of **C$_2$**, into two signals. Even though, this resulted in a quite distorted NMR spectrum, the majority of the peaks could be assigned to the corresponding protons by their chemical shifts and splitting as shown in Figure 2.

The identity of the cross-shaped monomer was further corroborated by the solid-state structure of **C$_1$**. Single crystals suitable for X-ray analysis were obtained by slow vapor diffusion of heptane into a saturated solution of **C$_1$** in toluene. The solid-state structure showed that **C$_1$** crystallizes as racemic mixture of both enantiomers, which arise from interlocking the axial twist of the di-ester side of the molecule ((*P*)-**C$_1$** is displayed in Figure 3). In the crystal packing each enantiomer is accompanied by one toluene molecule and the two quarter-phenyl rods open an angle of 73°.

The racemic mixture was separated into its enantiomers on a chiral stationary phase HPLC (IG-chiralpak, heptane/CH$_2$Cl$_2$: 40/60 v/v, supporting information Figure S4). The enantiomers were separated on analytical scale and circular dichroism (CD) measurements revealed that their spectra have perfect mirror image of the *Cotton* bands. DFT based simulation of the CD spectrum allowed to assign the first eluting sample as *P*- and the second eluting one as the *M*-enantiomer (Supporting information Figures S5 and S6).
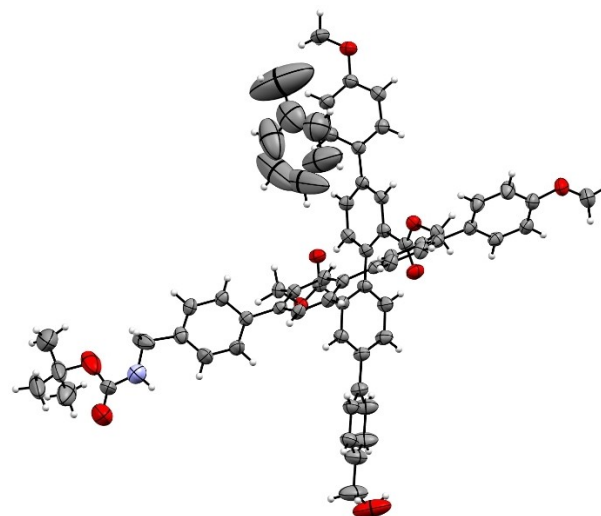
Figure 3. Solid-state structure of cross (P)-**C$_1$**, plotted as ORTEP plots with 50% probability. Plotted as single enantiomer for clarity.

Oligomerization

With the racemic monomer **C$_M$** in hand we investigated the imine-condensation based oligomerization (Figure 4A). Due to easier handling and improved storing stability of **C$_2$** in respect to **C$_M$**, **C$_M$** was freshly prepared prior to every oligomerization attempt via TFA mediated deprotection of the Boc group in dichloromethane. As we aimed for cyclic oligomers, the *Schiff*-base condensation was performed under (pseudo)-high dilution conditions favoring intra vs. inter molecular reactions. The outcome of imine based covalent organic framework synthesis

Chemistry–A European Journal

Research Article
doi.org/10.1002/chem.202402866

Chemistry
Europe
European Chemical
Societies Publishing
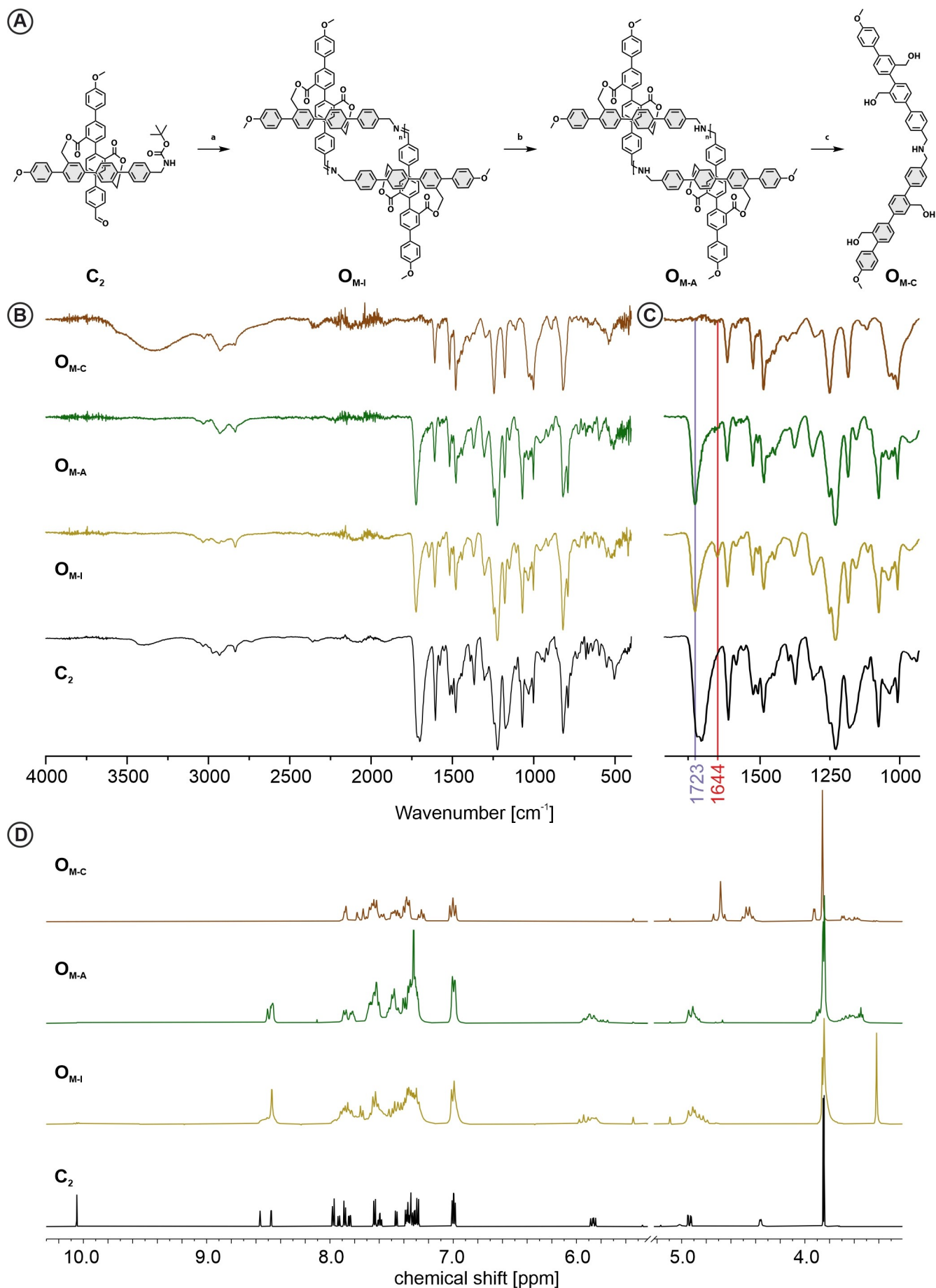
Figure 4. A) Synthesis scheme of imine condensation, reduction and template removal. Conditions a) i. TFA; CH$_2$Cl$_2$; r.t.; 1 h; ii) [c] 1 mmol/L; Na$_2$CO$_3$; CH$_2$Cl$_2$; r.t.; 24 h or TEA; THF; r.t.; 24 h; or TEA; CHCl$_3$; 60 °C; 24 h; b) NaBH(OAc)$_3$; B(OH)$_3$; CHCl$_3$; r.t.; 4 h; c) LiAlH$_4$; THF; 0 °C r.t.; 2 h. B,C) FT-IR (neat) and D) ¹H-NMR (CD$_2$Cl$_2$, r.t.) analysis of **C$_2$**, **O$_{M-I}$**, **O$_{M-A}$**, **O$_{M-C}$**, showing the appearance and disappearance of the characteristic signals corresponding to functional groups imine (1644 cm^{-1}; 8.5 and 4.84 ppm), ester (1723 cm^{-1}; 5.8 and 4.95 ppm), aldehyde (1697 cm^{-1}, 10.2 ppm), benzylic alcohol (–C**H$_2$**OH) (4.68; 4.45 ppm).

Chemistry–A European Journal

Research Article
doi.org/10.1002/chem.202402866

**Chemistry
Europe**
European Chemical
Societies Publishing

has been reported to depend strongly on reaction conditions like *e.g.* temperature and solvent.[18–21] Therefore, three different conditions, altering solvent, temperature and base were investigated.

As already reported for the fourfold functionalized molecular cross model compound, the *Schiff*-base condensation could simply be triggered by deprotonation of the benzylic ammonium.[16] In an initial attempt C_M was dissolved in a 100/1 CH_2Cl_2/TFA mixture and dropwise added to a suspension of sodium carbonate in CH_2Cl_2. Monitoring the reaction by matrix-assisted laser desorption-ionization mass spectrometry (MALDI-MS) displayed the gradual formation of dimeric, trimeric and tetrameric oligomers within the first 30 min (Supporting information, Figure S7), while after 20 h solely one peak at 1646 m/z was observed, pointing at the cyclic dimer as thermodynamically favored species. Very similar dynamic in the formation of oligomers was observed by MALDI-MS for adapted conditions using triethylamine (TEA) as base either in dry-tetrahydrofuran (THF) at room temperature (condition 2) or in chloroform (CHCl₃) at elevated temperature (condition 3). However, due to the absence of solid Na_2CO_3, conditions 2 and 3 enabled to observe that the initially transparent solutions turned turbid indicating the precipitation of material. The reaction product O_{M-I} was analyzed by *Fourier* transform infrared spectroscopy (FT-IR) and ¹H-NMR. The FT-IR spectrum of O_{M-I} is displayed in Figure 4B, and parts of it expanded in Figure 4C. A new peak at 1644 cm⁻¹, highlighted by a red line in the background of Figure 4C, is characteristic for the C=N imine stretch vibration. The comparison with the FTIR spectrum of C_2 shows the disappearance of the broad signals at about 1700 cm⁻¹ from the carbonyl (C=O) stretch vibration of the aldehyde and Boc protection group. Furthermore, the carbonyl vibration at 1723 cm⁻¹, which can be assigned to the ester, remains, pointing at almost full conversion of the monomer to oligoimine. This was further corroborated by ¹H-NMR analysis of O_{M-I} in CD_2Cl_2. The spectrum revealed that there was almost no residual aldehyde or amine protons (Figure 4D), while new peaks arise at 4.84 and 8.50 ppm corresponding to the chemical shift of the benzylic protons and the formed imine proton respectively. To gain more information about the distribution of the oligoimine mixture or about the dimension of the formed cyclic oligoimine respectively, ¹H-NMR Diffusion Ordered Spectroscopy (DOSY) was performed. The O_{M-I} mixture indicated a single higher order species with a diffusion coefficient of $7.703\cdot10^{-10}$ m²/s in CD_2Cl_2 at 25 °C (Supporting information, Figure S8). Comparison to the diffusion coefficient of C_2 (D = $9.52\cdot10^{-10}$ m²/s) indicated that the molecular weight ratio of O_{M-I}/C_2 equals 1.93 suggesting a dimeric structure. The interpretation was further supported by, HR-ESI-MS analysis displaying exclusively a signal of the cyclic-dimeric imine species. While the dissolved species was identified as the cyclic dimer, it is noteworthy that the solubility of the system is at the edge. Thus, a possible hypothesis for the observation of only the smallest molecular patch could be a very limiting poor solubility of larger oligomeric species. In other words, the formed higher order oligomers might not be soluble enough to be detected in the DOSY experiment as well as HR-ESI-MS. However, a variety

of imine-based covalent organic architectures have been reported to form the smallest possible cyclic structure as the thermodynamically most stable compound.[22–24] Thus the formation of the cyclic imine dimer is in line with these results and just complements the already existing examples.

To improve the stability of the cyclic oligomers, the reduction of the imines to the more stable amines was considered. A variety of conditions were attempted using either ethanol or methanol as proton source, resulting in non or poor conversion. A better suited method was found by adapting a solid-state procedure of Cho et al., where they used boric acid as proton source in the presence of sodium borohydride $NaBH_4$.[25] Instead of the required grinding we found that this reaction performs very well in CHCl₃ with sodium borohydride triacetoxy ($NaBH(OAc)_3$) as reducing agent, resulting in full conversion after 4 h of O_{M-I} to O_{M-A}. The transformation was indicated by the disappearance of the FT-IR signal at 1644 cm⁻¹ (Figure 4B and C) and can also be observed in the ¹H-NMR spectra of the compounds (Figure 4D). However, overlapping signals reduce to some extent the visibility. The multiplet of O_{M-I} at 4.84 ppm is from the benzylic protons attached to the imine nitrogen and shift upon reduction to O_{M-A} to 3.7–3.9 ppm, where they overlap with the methoxy protons. In the same region are the benzylic protons formed upon the reduction of the imine group, from which the proton disappears at about 8.5 ppm, where it overlapped with signals from the quarter-phenyls. Comparing the ratio of the integrated signals (Supporting info, Figure S9) shows that the combined methoxy and benzylic amine peak integrates to twenty in comparison to respective four and four for the benzylic ester protons of the cross structure, matching the expected ratio for a dimer as well as higher order cyclic oligomers. To further verify the attribution of the signals to their respective protons we compared the ¹H-NMR of model compounds **I** and **A**, which are provided in supporting information Figure S10. Here **I** and **A**, showed similar chemical shifts in the assigned regions for the imine proton, as well as the CH_2 protons of the benzylic- imine and amine respectively, corroborating our assignment. Analysis of O_{M-A} via HR-ESI-MS revealed again the presence of the dimeric patch as most intense main peak. However, also the mass signals of cyclic trimeric as well as tetrameric species could be identified. Even though their intensities were several orders of magnitude lower than the dimer signal, it showed that there are several molecular patches present at least in trace. Again, it is noteworthy that the reduction to O_{M-A} also resulted in a slightly higher solubility, such that this might also support the sudden visibility of (in traces) present higher cyclic oligomers by the analytical techniques.

The improved stability of the amine and the identification of higher order oligomers by mass spectrometry motivated attempts to isolate distinct sizes of molecular patches. However, neither, silica column chromatography, size exclusion chromatography (SEC) or high-performance liquid chromatography was successful. In all attempts, either multiple species eluted simultaneously or the species displayed extreme smearing as illustrated by the SEC chromatogram (Supporting information, Figure S11). Once again, the behavior is characteristic for

Chemistry–A European Journal

Research Article
doi.org/10.1002/chem.202402866

Chemistry Europe
European Chemical
Societies Publishing

macromolecules with low solubility such that the analysis of the composition of the cyclic oligomers is to some extent handicapped by the most likely varying solubility of the different sized oligomers. However, based on the analytical data, the main component in solution is the macrocyclic dimer.

Even so the separation of the cyclic oligomer O_{M-A} into individual components failed, we moved forward to the final proof of concept step. The cross-shaped target structure has been developed with the intention to be able to divide it into the two bars that are forming it. Interestingly, upon cleavage of the interlinking ester bridges the formed structure O_{M-C} consisting of a pair of amine interlinked quarterphenyl bars remains the same irrelevant of the dimensions of the cyclic oligomer O_{M-A}. To cleave the two ester bridges interconnecting the two quarterphenyl bars to the cross, O_{M-A} was exposed to lithium aluminum hydride ($LiAlH_4$) in anhydrous THF to provide O_{M-C}. The transformation was once again clearly visible in the FT-IR analysis of the reaction product, which showed the complete vanishing of the carbonyl signal, while the OH vibration (3300 cm^{-1}) of the benzylic alcohols appears. In the ^{1}H-NMR of O_{M-C} the absence of the characteristic diastereotopic protons of the center motive documented the cleavage of the template, while two new peaks arise at 4.45 ppm and 4.68 ppm which can be attributed to the benzylic CH_2 groups neighboring the alcohols. Here, the most up-field shifted signal can be attributed to the benzylic position formed from the former acid, which due to steric clash appears as a multiplet. Therefore, the more downfield shifted protons were assigned to the other benzylic pair.

In spite of the unsolved challenges to separate the individual cyclic oligomers, the formation of the final species, the interlinked bars O_{M-C}, which was characterized by ^{1}H-NMR, 2D-NMR and HRMS, after isolation via silica column chromatography, corroborates the success of the series of intended transformations: namely; the condensation to cyclic oligoimines, their reduction to cyclic oligoamines, and the template cleavage (Supporting information, page S111–S116).

On-surface Synthesis

The intention behind the cross-shaped monomer is to form extended monolayers by self-assembling at the flat air/water interface. An interesting question was thus the behavior of the bifunctional cross-shaped monomer C_M on a planar 2D support. And indeed, our initial hope to be able to resolve the molecular shape in such an experiment were even excelled. To study C_M on a surface, a high vacuum electrospray deposition (HV-ESD) was performed.[26,27] The monomer was deposited on an Au(111) surface maintained at room temperature from a CH_2Cl_2/TFA (99/1) solution. Non-contact atomic force microscopy (nc-AFM) was used to confirm the successful deposition (Supporting information, Figure S12). The large scale topography image reveals the presence of C_M concentrated around the step-edges, clusters or small chains of C_M and remaining solvent molecules aligned at the herringbone kinks. However, the resolution of the sub

molecular image did not allow to clearly identify the subunits of C_M.

With the intention to remove residual solvent molecules, the substrate was annealed at 110°C for 20 min. Upon that treatment, the majority of the individual monomers previously spread on the surface, started to coalesce in assemblies of longer linear oligomeric structures (displayed in Figure 5A), which was interpreted as the on-surface imine condensation of C_M to O_{M-I}. As visible in the topography of Figure 5A, extended linear structures are identified, with lengths up to 50 nm. It thus seems that the annealing under high vacuum favors the imine formation, probably pushing the condensation to its product by removal of the water molecules. The herringbone Au(111) surface reconstruction, visible together with the molecules
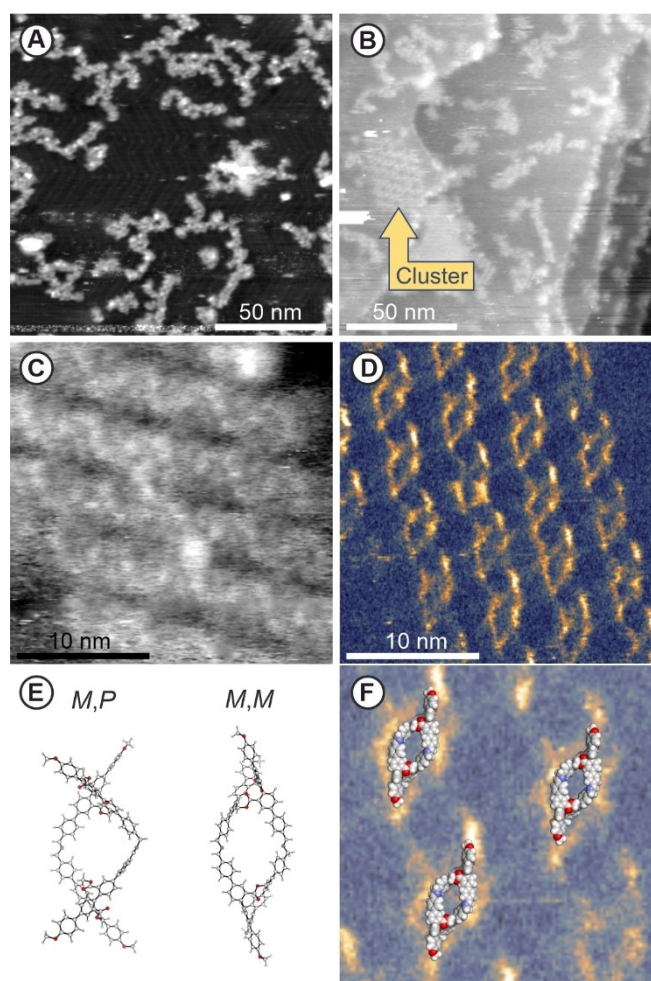
Figure 5. NcAFM images on electrospray deposited C_M, on an Au(111) surface after annealing at 110°C. A) Topography image showing linear polymeric structures and herringbone reconstruction of the gold surface B) Topography image, showing a highly organized cluster (mid-left). C) Topography and corresponding D) excitation of second eigenmode resonance on the cluster showing a repetitive pattern fitting the rhomboid shaped optimized geometry of (**M,P**)/(**M,M**)-$O_{M-I-dimer}$ in vacuo (BL3YP/6-31G(D) & BL3YP/6-21G) (E). F) (**M,M**)-$O_{M-I-dimer}$ overlaid with zoom in of the cluster.

parameters: f1 = 322 kHz. A) A1 = 5nm, Δf1 = -100 Hz. B) A1 = 3nm, Δf1 = -50 Hz. C,D) A1 = 8nm, Δf1 = -60 Hz, f2 = 2.3 MHz, A2 = 200pm.

Chem. Eur. J. **2024**, *30*, e202402866 (8 of 12)

© 2024 The Author(s). Chemistry - A European Journal published by Wiley-VCH GmbH

Chemistry–A European Journal

Research Article
doi.org/10.1002/chem.202402866

Chemistry Europe
European Chemical
Societies Publishing

(Supporting information, Figure S13), is a good indication of a clean surface after the removal of the solvent molecules.

Within the linear structures of various dimensions and shapes, also a cluster of highly ordered rhomboid shaped structures was observed (left side of Figure 5B). The zoomed second eigenmode topography on the cluster (Figure 5C) disclosed parallel rows in the substructure of the cluster. With the help of the simultaneously acquired dissipation image the cluster was resolved in more details, as shown in Figure 5D. Additional signals are visible in the supporting information Figure S14 to help to identify the cluster. We attribute the higher dissipative area to the skeleton of the molecules. The dissipation image shows the distortion in the rhombic structure where one corner is clearly pointing more out of plane, as well as that it seems to have a semi spiral like alignment on the surface. This advocates for the successful synthesis of cyclic dimer $O_{M-I-dimer}$.

The resolution of the excitation image (Figure 5D) even allowed to further identify the character of the formed macro-cyclicoligoimine dimer $O_{M-I-dimer}$. In Figure 5E the geometry optimized structures of two possible dimers are displayed, namely the (M,M)-$O_{M-I-dimer}$ as representative of a homochiral dimer made of enantiopure monomers, and (M,P)-$O_{M-I-dimer}$ as the meso form combining the enantiomers of different chirality. In Figure 5F, the M,M-dimer is overlaid with a zoom on the dissipation image of the rhombic structure, displaying pronounced structural as well as dimensional similarity. While the match of the structures suggest that the island consists exclusively of homochiral dimers, it does not allow to distinguish between M,M- and P,P-dimers. Most likely both homochiral dimers are present in comparable amounts. Even though the in vacuum optimized structures don't consider the surface influence, the similarity corroborates the assembly of cyclic dimeric structures on the Au(111) surface.

The successful deposition of the monomer and its on-surface condensation to oligoimines monitored and identified by HV-ESD and nc-AFM respectively, demonstrated both, the power and the potential of this technique. For our future plans, it allows to deposit monomers we intend to use for our molecular textile prematurely and to investigate its chemical behavior as well as structural features. In particular, the initiation of the imine condensation upon annealing might open new pathways towards the assembly of our intended 2D-structure. Thus, the combination of these techniques became very interesting tool to scout for suitable monomers and to investigate their condensation behavior, with potential similarities to the self-assembly and condensation behavior on the air/water interface.

Conclusion and Outlook

In the context of assembling a molecular textile, an in-solution strategy for the fabrication of molecular patches is presented. A bi-functional cross-shaped monomer C_M is developed, comprising as functional termini an aldehyde and a benzylic amine. Via ^{1}H-NMR and X-ray structure analysis the identity of the

monomer is corroborated as racemic mixture. The dimeric patch is obtained as main cyclic oligomer upon exposing the monomer to *Schiff*-base condensation conditions. Reversibility of the system is eliminated by reduction to the cyclic amines O_{M-A}. The crosses are divided into individual bars upon subsequent template cleavage transforming the cyclic amines into pairs of amine interlinked bars O_{M-C}. The success of the in-solution strategy corroborates the intended supramolecular function, the liberation of the covalently interlinked bars forming the crosses upon a chemical trigger.

Additionally, the monomer is exposed to a flat Au (111) surface via high vacuum electrospray deposition. On-surface imine condensation is achieved by annealing, resulting in the assembly of linear oligomers and a cluster of homochiral dimers. The structural identity of the dimeric patch is analyzed via nc-AFM, and excellent shape match with the calculated structures of a homochiral imine dimer (M,M)-$O_{M-I-dimer}$ is observed.

The findings not only show the potential of the cross architecture as covalently templated supramolecular synthon, but also provide an excellent fundament to benchmark the chemistry required to master the formation of molecular textiles. The established protocols and analysis methods are crucial in our-pursuit for the assembly of our desired mechanically interwoven 2D-material.

Experimental Section

General

All chemicals and solvents were purchased from Sigma Aldrich, Acros, Apollo Scientific, Alfa Aesar and Fluorochem and used as received. NMR solvents were obtained from CIL Cambridge Isotope Laboratories, Inc., Acros, Sigma-Aldrich, or Apollo Scientific. Dry solvents were used as crown capped and purchased from Acros and Sigma-Aldrich. Column chromatography was performed manually or on a Biotage Isolera using SilicaFlashR P60 from Silicycle with particle size of 40–63 μm (230–400 mesh) as stationary phase.TLC was performed with silica gel 60 F254 glass plates purchased from Merck. NMR experiments were performed on Bruker Avance III NMR spectrometers operating at 250, 400, 500 or 600 MHz proton frequencies. The instruments were equipped with a direct-observe 5 mm BBFO smart probe (250, 400 MHz), or an indirect-detection 5 mm BBI probe (500, 600 MHz) NMR. All probes were equipped with actively shielded z-gradients (10 A). The chemical shifts are reported in ppm relative to TMS or referenced to residual solvent peak and the J values are given in Hz. Infrared spectra were recorded neat with an ATR equipped Schimadzu IRTacer-100. High-resolution mass spectra (HR-MS) were measured with a Bruker Maxis 4G ESI-TOF instrument. CD measurements were performed on a JASCO J-1500 CD Spectrophotometer in a 1 cm quartz glass cuvette. For analytical HPLC, a Shimadzu LC-20AT HPLC was used, equipped with a diode-array UV/Vis detector (SPD–M20 A VP from Shimadzu, $\lambda = 200$–600 nm) and a column oven Shimadzu CTO-20AC. The used column for analytical separation on chiral stationary phase was a Chiralpak IG, 5 μm, 4.6×250 mm, Daicel Chemical Industries Ltd.

Chemistry–A European Journal

Research Article
doi.org/10.1002/chem.202402866

Chemistry Europe
European Chemical
Societies Publishing

Synthetic Procedures

Di-bromide 1: A 25 mL Schlenk tube was charged with boronic ester **3** (165 mg, 1 equiv.). iodine **2** (182 mg, 1 equiv.) and K_2CO_3 (104 mg, 3 equiv.). The solids were dispersed in a 10 mL THF/H_2O (4:1; v/v) mixture. The resulting suspension was degassed with argon followed by the addition of $PdCl_2(dppf)$ (14 mg, 7 mol%). The mixture was heated at 60°C for 5 h before cooled down to room temperature and filtered over a silica pad. The silica pad was flushed down with EtOAc and the filtrate was washed with H_2O. The organic layer was collected, dried with sodium sulfate and concentrated before subjected to Silica column chromatography using Cyclohexane:EtOAc (8:2 to 7:3; v/v) as eluent. The product was obtained as a white solid (222 mg, 82%) after stripping of the volatiles.

^{1}H-NMR: (500 MHz, CD_2Cl_2): δ 8.10–8.09 (m, 1H), 8.07 (s, 1H), 7.72–7.64 (m, 2H), 7.61–7.57 (m, 2H), 7.57–7.53 (m, 2H), 7.51–7.46 (m, 2H), 7.37–7.19 (m, 8H), 7.16–7.11 (m, 2H), 7.10–7.06 (m, 2H), 7.04–6.98 (m, 4H), 6.87–6.83 (m, 2H), 4.99–4.95 (m, 4H), 4.92 (s, 1H), 4.75 (s, 2H), 4.24 (d, $J=6.0$ Hz, 2H), 3.87 (s, 3H), 3.76 (s, 3H), 1.92 (s, 1H), 1.44 (s, 9H). ^{13}C-NMR {1H}: (126 MHz, CD_2Cl_2): δ 167.14, 167.00, 160.10, 159.64, 142.05, 140.92, 139.95, 139.22, 139.19, 138.94, 138.48, 135.34, 132.65, 132.58, 132.12, 131.96, 131.91, 131.74, 131.53, 131.45, 131.40, 131.30, 130.49, 130.32, 130.30, 130.12, 129.68, 129.51, 128.82, 128.47, 128.33, 127.76, 127.73, 127.51, 121.51, 121.11, 114.62, 114.13, 79.73, 65.14, 64.50, 64.44, 55.75, 55.64, 28.53. HR-ESI-MS (+): m/z calculated for $C_{61}H_{53}Br_2NO_9Na$ [M+Na]$^+$; 1124.1979 found 1124.1987.

Cross C$_1$: Dibromo **1** (210 mg, 0.19 mmol, 1 equiv.), B_2Pin_2 (117 mg, 0.46 mmol, 2.4 equiv.) and KOAc (112 mg, 1.14 mmol, 6 equiv.) were loaded into a 25 mL flame-dried *Schlenk* tube and cycled between vacuum and argon 3 times. Dry Dioxane (6 mL) was added and the mixture was degassed with argon for 15 min. $PdCl_2(dppf)$ (18 mg, 0.02 mmol, 0.1 equiv.) was added and the mixture was heated to 90°C. The reaction was tracked via LC–MS and after full consumption (3 h) of the starting material the reaction was cooled down to room temperature, filtered over a silica pad, flushed down with EtOAc and concentrated under reduced pressure. The concentrate was dissolved in 100 mL THF, followed by the addition of $PdCl_2(PPh_3)_2$ (67 mg, 0.095 mmol, 0.5 equiv.) and boric acid (59 mg, 0.95 mmol, 5 equiv.). The mixture was stirred vigorously for 15 min before KF (114 mg, 1.9 mmol, 10 equiv.) dissolved in 10 mL H_2O was added in one portion. The mixture was stirred for 16 h at room temperature open to the atmosphere, before it was filtered over silica and flushed down with THF. Organic volatiles were removed under reduced pressure and the remaining aqueous phase was extracted with EtOAc 3 times. The organic phases were combined, dried with sodium sulphate and concentrated under reduced pressure. The crude was purified by SiO_2 column chromatography using Cyclohexane and EtOAc as eluent, collecting the 2nd band. The obtained yellowish solid was dispersed in MeOH and the white precipitate was collected by filtration and dried, yielding the desired compound **C$_1$** as an off-white solid (115 mg, 64% over two steps).

^{1}H-NMR: (500 MHz, CD_2Cl_2): δ 8.51 (d, $J=2.0$ Hz, 1H), 8.47 (d, $J=2.0$ Hz, 1H), 7.87 (dd, $J=8.0$, 2.0 Hz, 1H), 7.83 (dd, $J=8.0$, 2.1 Hz, 1H), 7.72–7.67 (m, 2H), 7.66–7.62 (m, 2H), 7.61–7.56 (m, 2H), 7.46 (d, $J=8.3$ Hz, 2H), 7.41 (d, $J=8.0$ Hz, 1H), 7.39–7.28 (m, 11H), 7.02–6.97 (m, 4H), 5.89–5.84 (m, 2H), 5.03 (s, 1H), 4.94 (d, $J=9.1$ Hz, 1H), 4.91 (d, $J=9.0$ Hz, 1H), 4.74–4.70 (m, 2H), 4.36 (d, $J=6.1$ Hz, 2H), 3.85 (s, 3H), 3.84 (s, 3H), 1.87 (s, 1H), 1.46 (s, 9H). ^{13}C-NMR {1H}: (126 MHz, CD_2Cl_2): δ 166.29, 166.17, 160.03, 159.61, 156.27 144.77, 143.92, 141.29, 140.09, 140.06, 139.67, 139.31, 139.24, 139.20, 139.08, 139.04, 134.97, 134.87, 132.55, 132.36, 132.19, 132.04, 130.73, 130.64, 130.56, 130.27, 129.63, 129.61, 129.19, 128.48, 127.82,

127.71, 127.49, 125.92, 124.87, 124.82, 114.69, 114.24, 79.65, 65.10, 64.11, 64.03, 55.71, 44.59, 28.54. HR-ESI-MS (+): m/z calculated for $C_{61}H_{53}NO_9Na$ [M+Na]$^+$; 966.3603 found 966.3603.

Cross C$_2$: Cross **C$_1$** (60 mg, 0.064 mmol, 1 equiv.) was dissolved in dry dichloromethane (6 mL) and cooled down to 0°C. DMP (33 mg, 1.2 equiv.) was added portion wise while cooled and after full addition the mixture was allowed to warm to room-temperature. The mixture was tracked by TLC and upon full conversion after 1 h the mixture was quenched with sat. $NaHCO_3$ and sat. $NaHSO_3$. The aqueous phase was extracted with CH_2Cl_2 3 times and concentrated. The crude was plugged over a pad of silica (CH_2Cl_2:EtOAc 9:1) yielding the product as a white solid (52 mg, 86%).

^{1}H-NMR: (500 MHz, CD_2Cl_2) δ 10.05 (s, 1H), 8.57 (d, $J=2.0$ Hz, 1H), 8.48 (d, $J=2.1$ Hz, 1H), 7.97 (d, $J=8.1$ Hz, 2H), 7.92 (dd, $J=8.0$, 2.0 Hz, 1H), 7.88 (d, $J=8.2$ Hz, 2H), 7.84 (dd, $J=8.0$, 2.0 Hz, 1H), 7.66–7.62 (m, 2H), 7.60 (ddd, $J=8.1$, 6.6, 1.9 Hz, 2H), 7.46 (d, $J=8.0$ Hz, 1H), 7.40–7.27 (m, 12H), 7.03–6.97 (m, 4H), 5.87 (dd, $J=14.1$, 7.9 Hz, 2H), 5.03 (s, 1H), 4.94 (dd, $J=14.1$, 3.4 Hz, 2H), 4.36 (d, $J=6.2$ Hz, 2H), 3.85 (s, 3H), 3.84 (s, 2H), 1.46 (s, 9H). ^{13}C-NMR {1H}: (126 MHz, CD_2Cl_2) δ 192.11, 166.30, 165.94, 160.06, 159.62, 145.99, 143.60, 140.25, 139.65, 139.24, 139.21, 139.12, 138.99, 138.98, 136.05, 134.94, 134.79, 132.48, 132.43, 132.33, 131.88, 130.90, 130.75, 130.68, 130.60, 130.56, 130.33, 130.05, 129.63, 129.23, 128.48, 128.08, 128.05, 127.72, 127.64, 125.90, 124.91, 124.86, 114.71, 114.25, 79.78, 64.15, 64.12, 55.72, 44.58, 28.54. HR-ESI-MS (+): m/z calculated for $C_{61}H_{51}NO_9Na$ [M+Na]$^+$; 964.3456 found 964.3455.

Monomer C$_M$: Cross **C$_2$** (24 mg, 1 equiv.) was dissolved in 1 mL CH_2Cl_2 and 0.1 mL TFA was added, the mixture is stirred for 1 h. 5 mL toluene was added and the mixture was concentrated under reduced pressure yielding the product as the TFA salt (25 mg, quant.) as an off-white solid. **Reaction in NMR-Tube**: 3 mg of cross **C$_2$** was dissolved in 0.75 mL CD_2Cl_2 followed by the addition of 70 µL TFA-d. The tube was shaken until homogenous and ^{1}H-NMR spectra were recorded after several time intervals. After 1 h the spectra indicated full conversion towards the product.

^{1}H NMR (600 MHz, CD_2Cl_2:TFA-d 10:1) δ 9.98 (s, 1H), 8.60 (d, $J=2.0$ Hz, 1H), 8.53 (d, $J=2.0$ Hz, 1H), 8.11–8.06 (m, 2H), 7.97 (dd, $J=8.0$, 2.0 Hz, 1H), 7.92–7.86 (m, 3H), 7.67–7.58 (m, 4H), 7.54–7.39 (m, 6H), 7.34–7.26 (m, 6H), 7.09–7.03 (m, 4H), 5.84 (d, $J=14.4$ Hz, 2H), 5.08 (d, $J=14.4$ Hz, 1H), 5.00 (d, $J=14.4$ Hz, 1H), 4.40 (s, 2H), 3.94 (s, 3H), 3.93 (s, 3H).

^{1}H-NMR: (500 MHz, DMSO-d6): δ 10.07 (s, 1H), 8.54 (d, $J=2.1$ Hz, 1H), 8.42 (d, $J=2.1$ Hz, 1H), 8.22 (s, 3H), 8.11 (dd, $J=8.1$, 2.1 Hz, 1H), 8.06–7.99 (m, 4H), 7.96 (dd, $J=8.1$, 2.1 Hz, 1H), 7.75–7.67 (m, 4H), 7.60–7.56 (m, 2H), 7.55–7.48 (m, 3H), 7.40 (d, $J=8.0$ Hz, 1H), 7.38–7.32 (m, 4H), 7.25–7.18 (m, 2H), 7.09–7.03 (m, 4H), 5.77 (dd, $J=14.6$, 8.5 Hz, 2H), 5.00 (dd, $J=14.4$, 5.4 Hz, 2H), 4.16–4.09 (m, 2H), 3.81 (d, $J=5.1$ Hz, 6H).

^{13}C-NMR {1H}: (126 MHz, DMSO-d6): δ 192.76, 165.11, 164.85, 159.31, 158.84, 144.91, 144.34, 142.61, 139.15, 139.09, 137.83, 135.44, 134.20, 134.07, 131.01, 130.54, 130.28, 130.06, 129.16, 129.09, 127.87, 127.46, 127.03, 126.71, 124.74, 124.04, 114.56, 114.03, 63.92, 55.21, 55.19, 42.01. Signals: 192.76, 165.11, 164.85, 159.31, 144.91, 144.34, 142.61, 139.15, 139.09, 137.83, 134.20, 134.07, 131.01, 130.54, 127.03, 126.71, 124.74, 124.04, 63.92 are extracted from 2D-NMR. HR-ESI-MS (+): m/z calculated for $C_{56}H_{44}NO_7$ [M+H]$^+$; 842.3112, found 842.3120.

Synthesis of **2** and **3** are reported in the supporting information.

Chem. Eur. J. **2024**, *30*, e202402866 (10 of 12)

© 2024 The Author(s). Chemistry - A European Journal published by Wiley-VCH GmbH

Chemistry–A European Journal

Research Article
doi.org/10.1002/chem.202402866

Chemistry Europe
European Chemical
Societies Publishing

OligomerizationImine Condensation O_{M-I}

tlsb = 0%**Procedure 1: C_M** (1 equiv.) was dissolved in CH_2Cl_2:TFA (1 mmol/mL) and dropwise added to a dispersion of Na_2CO_3 (10 equiv.) in CH_2Cl_2. After full addition the mixture was allowed to stir for 24 h before the mixture was filtered over cotton and the filtrate was concentrated under reduced pressure, obtaining **O_{M-I}**.

Procedure 2: C_M (1 equiv.) was dissolved in dry-THF (1 mmol/L) and the mixture was stirred for 1 h at room-temperature. TEA (2 equiv.) was added and the resulting mixture was stirred for an additional 16 h. The volatiles were removed under reduced pressure and the solids were triturated with MeOH (3 times) to obtain **O_{M-I}**.

Procedure 3: C_M (1 equiv.) was dissolved in chloroform (1 mmol/mL) and the mixture was heated to 60 °C. Then TEA (2 equiv.) was added and the resulting mixture was stirred at 60 °C for 16 h. After cooling down MeOH (20 mL) was added and the insoluble **O_{M-I}** were collected via filtration. The solids were washed with an additional portion of MeOH.

Reduction O_{M-A}: O_{M-I} (1 equiv., calculated from **C_M** step 1), ground $B(OH)_3$ (20 equiv.) and $NaBH(OAc)_3$ (20 equiv.) were added to a round-bottom flask. Chloroform (5 mmol/L) was added and the resulting suspension was stirred for 4 h. The reaction was quenched with sat. $NaHCO_3$ and the mixture was concentrated under reduce pressure. The solids were washed with water 3 times followed by MeOH, obtaining **O_{M-A}** as the remaining solid.

Template cleavage O_{M-C}: O_{M-A} (5 mg) was dissolved in 2 mL dry-THF under argon atmosphere. The mixture was cooled before 1 M $LiAlH_4$ in THF (0.02 mL, 5 equiv.) was added carefully. The mixture was allowed to heat to room temperature and stirred for 3 h. The mixture was cooled on ice before it was quenched with some drops of water. The mixture was diluted with chloroform and excess Na_2SO_4 was added. The suspension was filtered of and the filtrate was concentrated. The crude was subjected to silica gel column chromatography (CH_2Cl_2:MeOH 93:7→9:1) collecting **O_{M-C}** as a white solid (1.2 mg, 22%). ^1H NMR (500 MHz, THF): δ 7.98 (dd, $J = 8.8, 1.7$ Hz, 2H), 7.90 (dd, $J = 6.2, 1.7$ Hz, 1H), 7.85 (d, $J = 1.7$ Hz, 1H), 7.69–7.66 (m, 2H), 7.65–7.60 (m, 4H), 7.57 (dd, $J = 7.8, 2.0$ Hz, 1H), 7.53–7.45 (m, 4H), 7.44–7.39 (m, 2H), 7.38–7.35 (m, 2H), 7.32 (d, $J = 7.9$ Hz, 1H), 7.30 (d, $J = 7.9$ Hz, 1H), 7.17 (ddd, $J = 11.4, 7.8, 4.0$ Hz, 2H), 7.04–6.94 (m, 4H), 4.58 (dd, $J = 9.0, 5.4$ Hz, 4H), 4.37 (q, $J = 4.8$ Hz, 4H), 4.18 (tt, $J = 9.6, 5.4$ Hz, 4H), 3.89 (d, $J = 3.9$ Hz, 4H), 3.82 (d, $J = 1.1$ Hz, 6H). ^{13}C-NMR (126 MHz, THF): (C-adjacent to H, subtracted from HMQC) δ 130.08, 129.88, 129.86, 129.71, 129.58, 129.30, 129.20, 128.55, 127.67, 127.59, 126.75, 126.45, 126.36, 126.00, 125.63, 124.86, 124.64, 124.30, 113.94, 113.30, 61.64, 61.38, 54.15, 52.50. HR-ESI-MS (+): m/z calculated for $C_{56}H_{52}NO_6$ $[M+H]^+$; 834.3789, found 834.3796.

High Vacuum Electrospray Deposition

The electrospray deposition is performed on samples kept at room temperature in ultra high vacuum conditions using a modified commercial system from molecular-spray, as already explained in.[26–30] The **C_M** molecules are dissolved in a CH_2Cl_2/TFA mixture (ratio 99/1). During the spray deposition, the pressure rose up to 5.0×10^{-8} mbar. Typical applied voltage is 1.2 kV for 10 min.

Au(111) Sample Preparation

Au(111) single crystal (Mateck GmbH) are prepared in UHV conditions with several cycles of Ar^+ sputtering and annealing at 750 K. Surfaces are imaged after clean preparation and herringbone reconstruction is observed for all surfaces.

Room Temperature ncAFM

Room temperature ncAFM measurement are performed with a home built non contact atomic force microscope operated with a Nanonis electronic RC4.5. PPP-QNCHR cantilevers (Nanosensor) are used as sensor (typical resonance frequencies of $f_1 = 320$ kHz, $f_2 = 2{,}3$ MHz and oscillation amplitudes $A_1 = 2$–10 nm, $A_2 = 200$ pm for first and second eigenmode respectively). Cantilever preparation consisted of an annealing for 1 h at 400 K followed by Ar^+ sputtering for 90 s at 700 eV. During experiments, the base pressure of the UHV system was 2.0×10^{-11} mbar. Data are analyzed using the Gwyddion software.[31]

Supporting Information Summary

The Supporting Information comprises the synthetic protocols and the characterization of the compounds, physicochemical analyses, oligomerization protocols and analyses including simpler model compounds detailed, geometry optimization and characterization and crystallographic data. Deposition Numbers 2371751 (**3**) and 2374177 (**C_1**) contain the supplementary crystallographic data. These data are provided free of charge by the joint Cambridge Crystallographic Data Centre and Fachinformationszentrum Karlsruhe Access Structures service. The authors have cited references within the Supporting Information.

Conflict of Interests

The authors declare no conflict of interest.

Data Availability Statement

The data that support the findings of this study are available in the supplementary material of this article.

[1] S. Seema, *Textbook of Fabric Science, Fourth Edition: Fundamentals to Finishing*, PHI Learning Pvt. Ltd. **2022**, New Delhi .
[2] A. Di Silvestro, M. Mayor, *Chimia* **2019**, *73*, 455.
[3] Z.-H. Zhang, B. J. Andreassen, D. P. August, D. A. Leigh, L. Zhang, *Nat. Mater.* **2022**, *21*, 275–283.

[4] G. Gil-Ramírez, D. A. Leigh, A. J. Stephens, *Angew. Chem. Int. Ed.* **2015**, *54*, 6110–6150.

[5] S. Mena-Hernando, E. M. Pérez, *Chem. Soc. Rev.* **2019**, *48*, 5016–5032.

[6] A. Godt, *Eur. J. Org. Chem.* **2004**, *2004*, 1639–1654.

[7] F. L. Thorp-Greenwood, A. N. Kulak, M. J. Hardie, *Nat. Chem.* **2015**, *7*, 526–531.

[8] Y. Liu, Y. Ma, Y. Zhao, X. Sun, F. Gándara, H. Furukawa, Z. Liu, H. Zhu, C. Zhu, K. Suenaga, P. Oleynikov, A. S. Alshammari, X. Zhang, O. Terasaki, O. M. Yaghi, *Science* **2016**, *351*, 365–369.

[9] G. Schill, A. Lüttringhaus, *Angew. Chem. Int. Ed. Engl.* **1964**, *3*, 546–547.

[10] M. D. Cornelissen, S. Pilon, J. H. Van Maarseveen, *Synthesis* **2021**, *53*, 4527–4548.

[11] S. Duda, A. Godt, *Eur. J. Org. Chem.* **2003**, *2003*, 3412–3420.

[12] P. W. Fritz, A. Coskun, *Chem* **2023**, *9*, 2363–2365.

[13] D. P. August, R. A. W. Dryfe, S. J. Haigh, P. R. C. Kent, D. A. Leigh, J.-F. Lemonnier, Z. Li, C. A. Muryn, L. I. Palmer, Y. Song, G. F. S. Whitehead, R. J. Young, *Nature* **2020**, *588*, 429–435.

[14] Z. Wang, A. Błaszczyk, O. Fuhr, S. Heissler, C. Wöll, M. Mayor, *Nat. Commun.* **2017**, *8*, 14442.

[15] U. Lewandowska, W. Zajaczkowski, S. Corra, J. Tanabe, R. Borrmann, E. M. Benetti, S. Stappert, K. Watanabe, N. A. K. Ochs, R. Schaeublin, C. Li, E. Yashima, W. Pisula, K. Müllen, H. Wennemers, *Nat. Chem.* **2017**, *9*, 1068–1072.

[16] C. C. E. Kroonen, A. D'Addio, A. Prescimone, O. Fuhr, D. Fenske, M. Mayor, *Helv. Chim. Acta* **2023**, *106*, e202200204.

[17] I. J. S. Fairlamb, *Chem. Soc. Rev.* **2007**, *36*, 1036–1045.

[18] J. L. Segura, M. J. Mancheño, F. Zamora, *Chem. Soc. Rev.* **2016**, *45*, 5635–5671.

[19] M. J. MacLachlan, *Pure Appl. Chem.* **2006**, *78*, 873–888.

[20] M. Grigoras, C. O. Catanescu, *J. Macromol. Sci. Part C Polym. Rev.* **2004**, DOI: 10.1081/MC-120034152.

[21] C. M. Taylor, N. L. Kilah, *J. Incl. Phenom. Macrocycl. Chem.* **2022**, *102*, 543–555.

[22] D. Xu, R. Warmuth, *J. Am. Chem. Soc.* **2008**, *130*, 7520–7521.

[23] M. Kaik, J. Gawroński, *Org. Lett.* **2006**, *8*, 2921–2924.

[24] M. E. Belowich, J. F. Stoddart, *Chem. Soc. Rev.* **2012**, *41*, 2003–2024.

[25] B. T. Cho, S. K. Kang, *Tetrahedron* **2005**, *61*, 5725–5734.

[26] A. Hinaut, R. Pawlak, E. Meyer, T. Glatzel, *Beilstein J. Nanotechnol.* **2015**, *6*, 1927–1934.

[27] A. Hinaut, T. Meier, R. Pawlak, S. Feund, R. Jöhr, S. Kawai, T. Glatzel, S. Decurtins, K. Müllen, A. Narita, S.-X. Liu, E. Meyer, *Nanoscale* **2018**, *10*, 1337–1344.

[28] Molecularspray, http://molecularspray.co.uk/, accessed on 02-01-2024.

[29] S. Scherb, A. Hinaut, R. Pawlak, J. G. Vilhena, Y. Liu, S. Freund, Z. Liu, X. Feng, K. Müllen, T. Glatzel, A. Narita, E. Meyer, *Commun. Mater.* **2020**, *1*, 1–7.

[30] A. Hinaut, S. Scherb, S. Freund, Z. Liu, T. Glatzel, E. Meyer, *Beilstein J. Nanotechnol.* **2021**, *12*, 552–558.

[31] "Gwyddion–Free SPM (AFM, SNOM/NSOM, STM, MFM, …) data analysis software," can be found under http://gwyddion.net/, accesed on 02-01-2024 .